

UDC 544.032.4+544.015

DOI: 10.15372/CSD20170604

## Nanostructured Composites, Such as Porous Carbon Matrixes – Thermolysis Products of $\text{Co}(\text{N}_3)_2$

YU. A. ZAKHAROV<sup>1,2</sup>, N. M. FEDOROVA<sup>2</sup>, G. YU. SIMENYUK<sup>1</sup>, V. M. PUGACHEV<sup>2</sup>, V. G. DODONOV<sup>2</sup><sup>1</sup>*Institute of Coal Chemistry and Material Science, Siberian Branch, Russian Academy of Sciences, Kemerovo, Russia**E-mail: zaharov@kemsu.ru*<sup>2</sup>*Kemerovo State University, Kemerovo, Russia*

(Received October 01, 2017; revised November 13, 2017)

### Abstract

The paper considers properties of nanostructured composites based on porous carbon matrixes filled with thermolysis products of cobalt azide species pre-synthesised in matrix pores. Porous carbon materials of Carbonizate 3 and Cemerite 8 type were used as matrixes. The research was performed by X-ray diffraction, X-ray fluorescence analysis, and small angle X-ray scattering (SAXS) techniques. According to X-ray diffraction data, decomposition products of  $\text{Co}(\text{N}_3)_2$  in the explosive mode using Carbonizate 3 matrix are cobalt metal and  $\text{CoO}$ , while in case of Cemerite 8, the main product of thermal decomposition is  $\text{Co}_3\text{O}_4$  spinel. The sizes of three registered groups of inhomogeneities observed in carbon matrixes during composite preparation lie in the region of 1–3, 6–18, and 160–300 nm, as demonstrated by the research of matrixes and a composite based on Carbonizate 3 by the SAXS method. Electrochemical properties of the resulting nanocomposite material were explored. The introduction of cobalt oxide into carbon matrix resulted in an increase in the electrical capacitance of the composite electrodes, as demonstrated. Capacitance increase is due to pseudocapacitance of cobalt oxides owing to reversible redox processes with the involvement of cobalt oxide hydroxide phases that are generated during cell charge/discharge.

**Keywords:** cobalt, cobalt azide, carbon matrix, nanostructured composite, supercapacitor

### INTRODUCTION

Lately, issues of efficient preparation, preservation, and use of energy have acquired increasing relevance. In this regard, modernization of systems for accumulation and storage of electric energy is of great importance. The progress in the area of enhancing performance related to this type of supercapacitors (SC) allows solving technology and energy issues [1, 2]. It is known that capacitive characteristics, specific power, stability under charge/discharge conditions and other functional characteristics of SC primarily

depend on the properties of electrode materials (EM) used therein. Electrode materials based on nanostructured heterophase composites (NC) consisting of highly porous electroconductive substrates (matrixes) with electrochemically active substances supported on them (usually, individual or mixed oxides, or transition and noble metal hydroxides) are related to a series of the most promising. Carbon materials of the type of graphene, thermally expanded graphite, C nanotubes, *etc.* are most often used as matrixes. The electric capacitance of these electrode materials includes double electric layer capacity

at the C matrix/electrolyte borderline and so-called pseudocapacitive component, *i.e.* the result of the progression of electrochemical processes over nanoparticles that are found in contact with the matrix of oxides (hydroxides). Herewith, it is important to provide a good (conducting) contact between filler and matrix species, and also the absence of pore blocking by them.

Promising precursors for obtaining transition metals (or their oxides) that fill in composites are azides, at the decomposition of which products not contaminated with side compounds, are generated. Degradation of azides in various reactions of solid phase decomposition of metal azides (thermolysis, radiolysis, *etc.*) may proceed depending on conditions in both slow and micro-explosive modes. This would allow obtaining metal or oxide fillers in both the external surface and pores of carbon matrixes during decomposing azide sub-micro (nano) size particles located in the surface and matrix pores that are in good contact with them.

Earlier, there had been demonstrated an opportunity to develop nanocomposite electrode materials for supercapacitors on the ground of the carbon matrix and cobalt oxide generated by thermal decomposition of cobalt azide [3].

The present paper presents the results concerning the effect of the type of carbon matrixes on the phase composition and dispersion characteristics of thermal decomposition products of  $\text{Co}(\text{N}_3)_2$  precipitated in pores of these matrixes. Additionally, electrochemical measurement results by methods of cyclic voltammetry (CV) and chronopotentiometry of the resulting composition material are given.

## EXPERIMENTAL

To obtain NC, porous carbon materials Carbonizate 3 (C3) with  $S_{\text{sp}} = 1110 \text{ m}^2/\text{g}$ , and  $V_{\Sigma} = 0.750 \text{ cm}^3/\text{g}$ ,  $V_{\text{micro}} = 0.310 \text{ cm}^3/\text{g}$  and Cemerite 8 (C8) with  $S_{\text{sp}} = 2040 \text{ m}^2/\text{g}$ , and  $V_{\Sigma} = 2.650 \text{ cm}^3/\text{g}$ ,  $V_{\text{micro}} = 0.091 \text{ cm}^3/\text{g}$  synthesised and characterized at the Institute of Coal Chemistry and Material Science of the Federal Research Center of Coal and Coal Chemistry SB RAS (Kemerovo) [4, 5] were used. The Cemerite matrix (C8) is the product of high-temperature (to 1000 °C) carbonization of analytically pure

hydroquinone – furfural mixtures. The Carbonizate (C3) matrix was synthesized from coal (Shestaki deposit, Kuznetsk coal basin) oxidized under natural conditions by hard alkaline treatment under mechanical activation conditions followed by high-temperature carbonization (after thorough washing from KOH and impurities). To prepare reagent solutions, analytically pure  $\text{CoCl}_2 \cdot 6\text{H}_2\text{O}$  and  $\text{NaN}_3$  were used.

X-ray fluorescence and X-ray diffraction measurements were carried out on a Difreil 401 diffractometer using iron radiation ( $\lambda K_{\alpha} = 1.9373 \text{ \AA}$ ) with the built-in energy dispersive Amptek XR-100CR detector.

The small angle X-ray scattering (SAXS) measurements were performed using a KRM-1 diffractometer in iron characteristic radiation by the method of counting pulses at points in the  $0.002\text{--}0.35 \text{ \AA}^{-1}$  range. Particle size distribution functions were computed in the approximation of homogeneous spheres according to SAXS curves.

Electrocapacitance measurements were carried out in a two-electrode asymmetric electrochemical cell using a Parstat 4000 potentiostat/galvanostat. Nafion was used as the separator, a 6 M KOH solution – as the electrolyte. A nanostructured composite was the working electrode, C3 carbon matrix – the counter electrode.

A nanostructured composite material was prepared proceeding from the calculated metal content in the material (10 and 40 %). Matrix sample was placed into a weighing bottle, an aqueous cobalt (II) chloride solution with a predetermined concentration was added and the mixture was kept for 1 h, after which the resulting composite was transferred onto filter paper and rinsed with distilled water. After washing, composites were dried over filters under normal conditions until constant mass. To obtain NC, carbon matrix with embedded cobalt azide was exposed to the thermal treatment. Composite degradation was carried out in a ceramic crucible heated to 220 °C.

## RESULTS AND DISCUSSION

The resulting composite samples contain only trace amounts of impurities except for  $\text{Cl}^-$ , the removal of which during washing

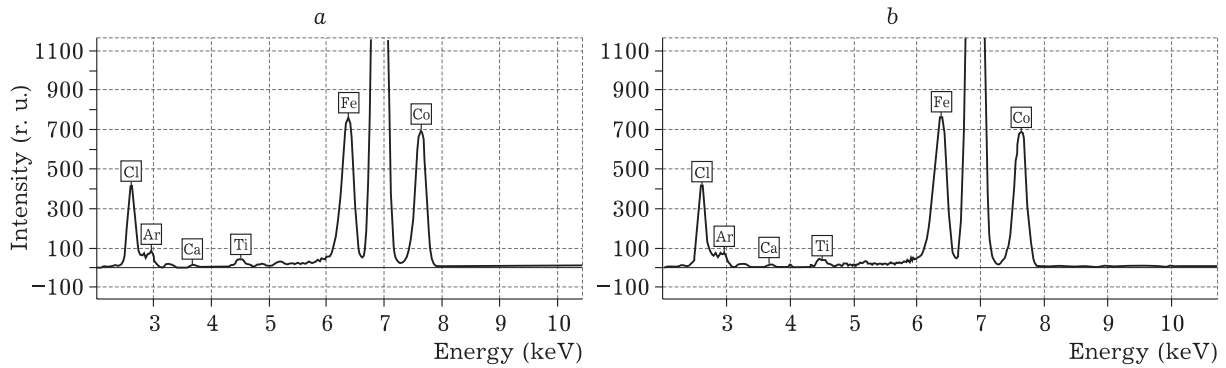


Fig. 1. X-ray fluorescence spectra of  $\text{Co}(\text{N}_3)_2/\text{C}3$  (a) and  $\text{CoN}_6/\text{C}8$  (b) composite materials.

is complicated, as demonstrated by X-ray fluorescence spectra (Fig. 1).

Samples of nanocomposites with a large content of cobalt azide on C3 and C8 matrixes were selected for thermal decomposition. The progression of thermolysis of  $\text{Co}(\text{N}_3)_2$  over various matrixes with different rates and the generation of various final products is untrivial. Azide thermodecomposition over C3 coal matrix occurs at  $t \sim 150^\circ\text{C}$  with a soft explosion, over C8 matrix at  $t \sim 200^\circ\text{C}$  – with even a softer blast. Phase composition of thermolysis products is different (Fig. 2). The main products of thermolysis of cobalt azide over C3 matrix are cobalt metal with hexagonal (reflexes near  $53.1, 57.2, 60.9^\circ$ ) and cubic (reflexes near  $56.5, 66.2^\circ$ ) structures. Cobalt (II) oxide,  $\text{CoO}$ , ( $46.4, 54.1, 80.0^\circ$ ) is also registered; a very small amount of  $\text{Co}_3\text{O}_4$  may also be present.

The main product of decomposition of cobalt azide over C8 matrix is spinel (reflexes near

$46.8, 57.2, 77.0, 85.3^\circ$ ),  $\text{CoO}$  ( $54.1, 80.0^\circ$ ) and the presence of cubic cobalt ( $56.5^\circ$ ) in small amounts is probable.

The SAXS spectra allow observing three groups of inhomogeneities in carbon matrixes: in 2–3, 6–18, and 160–300 nm range (Fig. 3 gives typical results for C3 matrix). Comparison of these data with study results of the porous structure of matrixes by low-temperature nitrogen sorption technique allows referring these inhomogeneities to micro(submeso-), meso-, and macropores, respectively [6]. From the results obtained it follows that both  $\text{Co}(\text{N}_3)_2$  crystallites in  $\text{Co}(\text{N}_3)_2$  and species of thermal decomposition products (which is natural) are generated in matrix pores, since the profiles of size density distribution functions (SDDF) are qualitatively similar for matrixes and composites: additional modes in SDDF of composites related to the generation of azide species outside the pores are not observed. Similar morphology (the for-

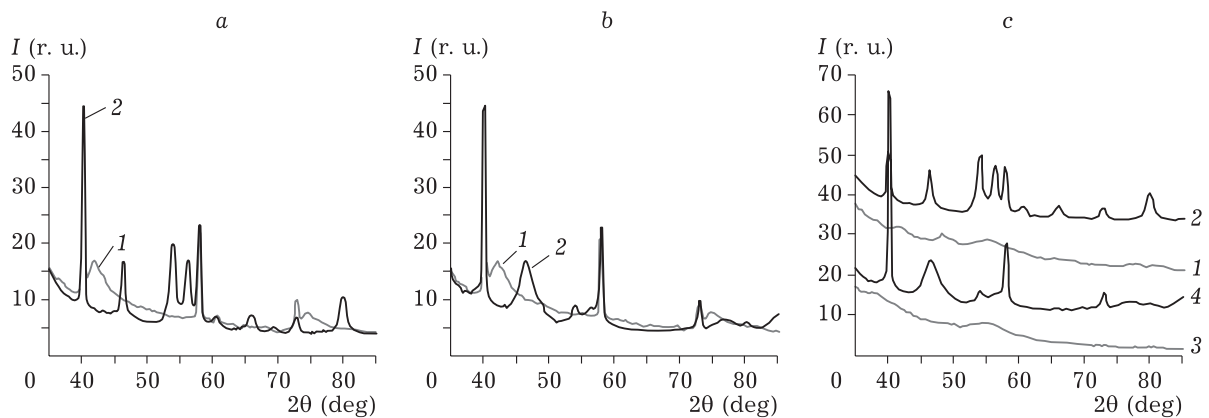


Fig. 2. Diffraction patterns of composite materials: a – initial composite  $\text{Co}(\text{N}_3)_2/\text{C}3$  (1) and  $\text{Co}^0, \text{CoO}/\text{C}3$  composite (2); b – initial  $\text{Co}(\text{N}_3)_2/\text{C}8$  composite (1) and  $\text{Co}_3\text{O}_4/\text{C}8$  composite (2); c – C3 matrix (1),  $\text{Co}^0, \text{CoO}/\text{C}3$  samples (2), C8 matrix (3);  $\text{Co}_3\text{O}_4/\text{C}8$  (4).

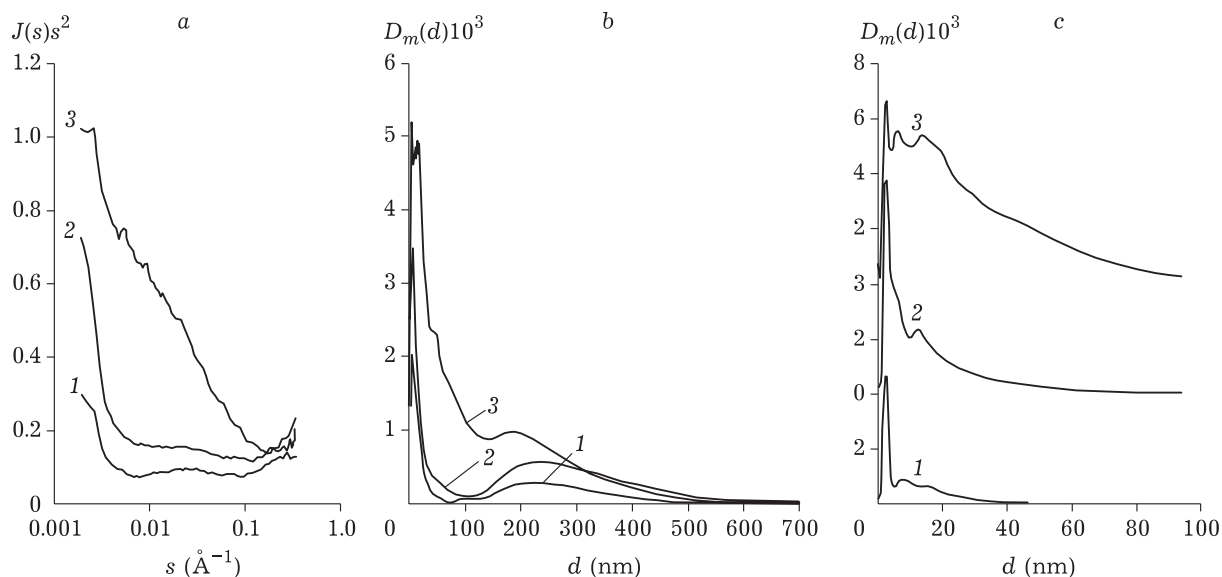


Fig. 3. Experimental SAXS spectra for a pure matrix in the studied samples of  $\text{Co}(\text{N}_3)_2/\text{C3}$  nanocomposites (a), mass functions of size inhomogeneity distribution for pure C3 matrix and samples of  $\text{Co}(\text{N}_3)_2/\text{C3}$  nanocomposites in submicron (b) and nanoscale (c) areas: 1 – pure Carbonizate matrix C3; 2 –  $\text{Co}(\text{N}_3)_2/\text{C3}$ ; 3 –  $\text{Co}(\text{N}_3)_2/\text{C3}$ , thermal treatment at  $\approx 150^\circ\text{C}$  that resulted in microexplosion.

mation of filler species primarily in pores of C8 and C3 matrixes) is typical for nanoparticles of other fillers ( $\text{Ni}(\text{OH})_2$ ,  $\text{Co}(\text{OH})_2$ ,  $\text{Mn}_x\text{O}_y$ , Au, and Ag) and NC based on these matrixes obtained by other methods [7–9]. Assessment of  $\text{Co}(\text{N}_3)_2$  crystallite sizes (nanometer units) according to broadening of X-ray reflections (see Fig. 2) in comparison with pore sizes of carbon matrixes (Fig. 3, c) confirms an opportunity to locate azide species even in submesopores. This is also in agreement with the nature of a change of SDDF – a significant increase in intensities of modes as a consequence of filling the pores with nanoparticles of  $\text{Co}(\text{N}_3)_2$  (NC  $\text{Co}(\text{N}_3)_2/\text{C}$  NC) or with Co and cobalt oxide (Co, CoO, and  $\text{Co}_3\text{O}_4/\text{C}$  NC) with electron density values significantly higher than in carbon.

Alongside with an increase in the intensities of modes for inhomogeneities generated on the basis of meso- and macropores the total decrease in their sizes is notable. The latter is expressed more substantially for NC of thermolysis product of  $\text{Co}(\text{N}_3)_2/\text{C}$  (see Fig. 3, b, c). This is certainly related to a decrease in the size of inhomogeneities (remaining unfilled with  $\text{Co}(\text{N}_3)_2$  crystallites of a part of pore volumes or products of its thermal decomposition) after azide is generated in crystallite pores *via* an

exchange reaction of dissolved  $\text{NaN}_3$  and  $\text{CoCl}_2$  followed by decomposition of  $\text{Co}(\text{N}_3)_2$ . As for submesopores, they are almost completely filled with filler crystallites or blocked by them. Herewith, the sizes of inhomogeneities are barely changing.

Joint consideration of the SAXS and XPA results and the data regarding the porous structure of the used matrixes (see above and in more details in [7–9]) allows discussing probable causes of the observed differences in phase compositions of decomposition products of  $\text{Co}(\text{N}_3)_2$  over different matrixes. The C8 matrix has a substantially greater porosity, therefore, during generating  $\text{Co}(\text{N}_3)_2/\text{C}$  nanocomposites with the same azide content and close crystallite sizes, judging by broadening of reflexes and crystallite sizes (see Fig. 2), their amount in one pore should be substantially lower than that in the pore of C8 matrix (right up to a probable situation, such as one pore – one  $\text{Co}(\text{N}_3)_2$  crystal. Herewith, the improvement of heat removal conditions causes the observed rise in the temperature of non-isothermal decomposition of azide in linear heating mode.

The primary product of decomposition of  $\text{Co}(\text{N}_3)_2$  is cobalt [10]. Cobalt oxides are oxidation products of low-dimensional metal

species. Thermolysis of  $\text{Co}(\text{N}_3)_2$  nanocrystallites distributed in a large number of pores of C8 (in other words, with a lower fraction of their filling) is carried out under better heat removal conditions at high temperatures and in the presence of a larger volume of oxygen. That creates conditions for deeper oxidation of cobalt nanoparticles.

On the other hand, thermolysis of a large number of nanocrystallites in each C3 matrix pore (*i.e.* under conditions of high filling pores by them) proceeding at lower temperatures and under conditions of deficiency of oxygen contained in pores for deep oxidation leads to incomplete and superficial oxidation (to  $\text{CoO}$ ) of the metal product.

In view of the above, the sizes of  $\text{Co}_3\text{O}_4$  species generated during oxidation of cobalt product of thermal decomposition of single

$\text{Co}(\text{N}_3)_2$  crystals in C8 pores are substantially lower than those of  $\text{Co}^0$  and  $\text{CoO}$  generated during transformations of  $\text{Co}(\text{N}_3)_2$  crystallites in C3 pores and comparable with the dimensions of azide species (see Fig. 2).

It is worth noting that during thermal azide decomposition cobalt is generated as a mixture of species with low-temperature hexagonal close-packed (HCP) and high-temperature face-centered cubic (FCC) structures. The phase transition temperature in massive cobalt is  $420^\circ\text{C}$ ; however, it substantially reduced with decreasing crystal sizes [11], so that the fraction of the HCP phase during preparing crystals with a size of about 10 nm may be 90 %. Therefore, the observed effect may be a consequence of summation of cobalt particles nanodimensionality generated during decomposition of  $\text{Co}(\text{N}_3)_2/\text{C3}$  (from broadening

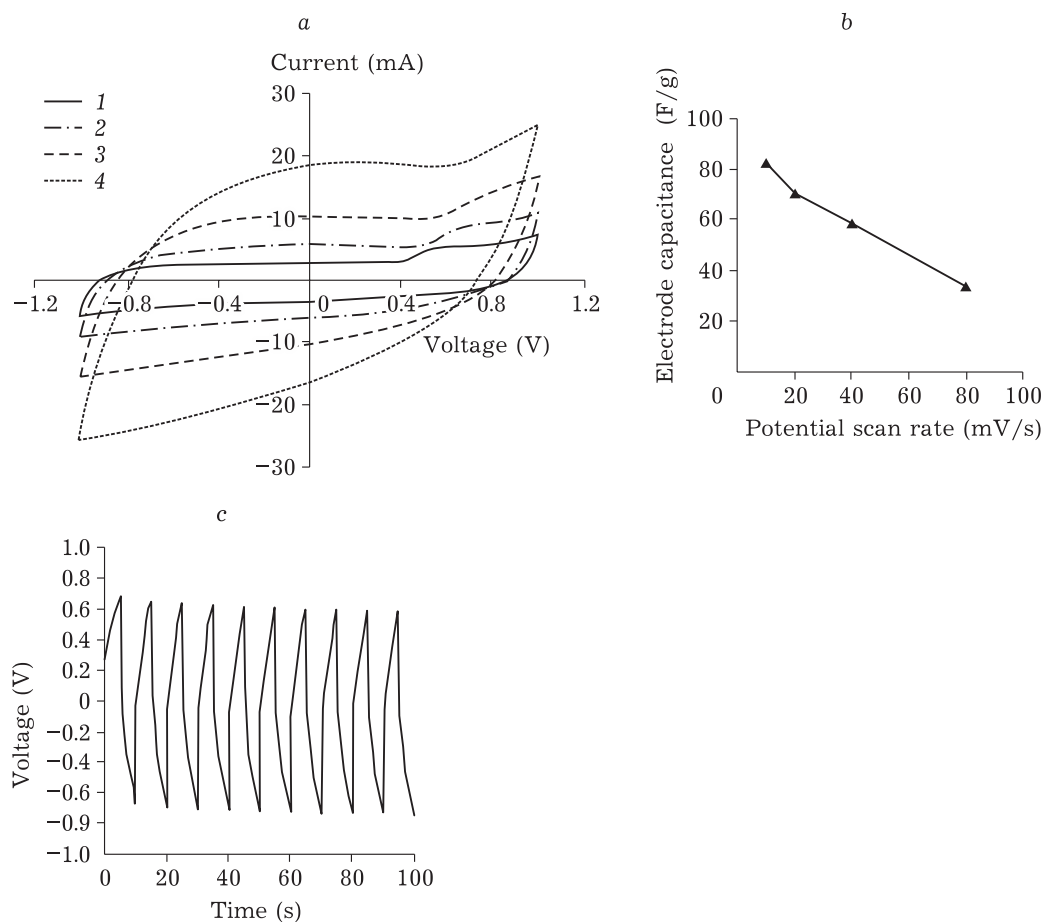


Fig. 4. Results of electrochemical studies of a supercapacitor with the working electrode based on  $\text{Co}^0, \text{CoO}/\text{C3}$ : a – CV curves in the potential window from  $-1$  to  $+1$  V at indicated potential scan rates 10 (1), 20 (2), 40 (3), 80 (4) mV/s; b – capacity of composite electrode materials versus potential scan rate; c – charge/discharge curves at the constant current strength.

of reflexes at about 20 nm in Fig. 2) and elevated temperatures (decomposition mode as a soft explosion at 150 °C). The generation of trace amounts of cobalt during decomposition of  $\text{Co}(\text{N}_3)_2/\text{C8}$  as the HCC phase is a consequence of higher decomposition temperatures.

The results of the study of NC  $\text{Co}, \text{CoO}/\text{C3}$  (Co content is ca. 40 %) by methods of CV and galvanostatic charge-discharge presented in Fig. 4, a, c.

The electrical capacitance was computed according to the area limited by CV curves according to the formula

$$C_c = q/(Um),$$

where  $C_c$  – cell capacity, F/g;  $q$  – accumulated charge in the cell, C (area in C – in the chart);  $m$  – mass, g;  $U$  – potential difference, V.

Electrode capacity was computed by the formula

$$1/C_c = 1/C_{we} + 1/C_{fe}$$

where  $C_{we}$  – working electrode capacity,  $C_{fe}$  – flow-through electrode capacity.

Cell capacity ( $C$ ) and equivalent series (internal) resistance ( $R_{\text{ESR}}$ ) were calculated by the common method according to galvanostatic discharge curves.

Figure 4, a gives CV curves of asymmetric supercapacitor cell with the working electrode based on  $\text{Co}^0, \text{CoO}/\text{C3}$  composite. It can be seen that the shape of CV curves is not rectangular, which is typical for electrodes accumulating charge at the expense of the generation of the electric double layer. The nature of the curves points to the progression of redox processes with the involvement of oxide hydroxide phases of cobalt (II).

The electric capacitance of  $\text{Co}^0, \text{CoO}/\text{C3}$  EM was computed based on the acquired CV curves. Figure 4, b gives the results.

The nanocomposite material has a relatively high capacity. The latter drops during increasing potential scan rate, which is typical for the majority of electrode materials. This may be due to ion diffusion limitations in pores or the kinetic retardation of electrochemical redox processes.

The electric capacitance of the composite electrode material and the  $R_{\text{ESR}}$  were 40 F/g and were 12 Om, respectively.

## CONCLUSION

Thus, nanostructured composite materials consisting of nanoscale  $\text{Co}_3\text{O}_4$  particles or a mixture of cobalt species and CoO products of thermal decomposition of cobalt azide in pores of carbon matrixes of two types were obtained. Phase and chemical compositions of fillers depend on the type of the carbon matrix used, which is related to the porous structure of matrixes. The composites may be used in developing electrode materials of supercapacitors, as demonstrated by electrochemical studies.

## REFERENCES

- 1 Gonzalez A., Goilelea E., Barrena A., Mysyk R., *Renewable and Sustainable Energy Reviews*. 2016. Vol. 58. P. 1189–1206.
- 2 Shan Y., Gao L., *Material Chemistry and Physics*. 2007. Vol. 103. P. 206–210.
- 3 Voropay A. N., Fedorova N. M., Zakharov Yu. A., Pugachev V. M., Dodonov V. G., Surovikin Yu. V., Ivanov A. V., *Chem. Sust. Dev*. 2016. Vol. 24, No. 2. P. 239–245.
- 4 Manina T. S., Fedorova N. I., Ismagilov Z. R., *Koks i Khimiya*. 2016. No. 7. P. 27–30.
- 5 Barnakov Ch. N., Samarov A. V., Shikina N. V., Yakubik D. G., *Chem. Sust. Dev*. 2015. Vol. 23, No. 2. P. 219–223.
- 6 Karnaukhov A. P. Adsorbtsiya. Tekstura Dispersnykh i Poristykh Materialov, Novosibirsk, Nauka, Sibirskoe otdelenie RAN, 1999. 470 p.
- 7 Zakharov Yu. A., Simenyuk G. Yu., Manina T. S., Barnakov C. N., Pugachev V. M., Podonov V. G., Pavelko N. V., *Nanotechnologies in Russia*. 2015. Vol. 10, No. 5–6. P. 388–399.
- 8 Simenyuk G. Yu., Zakharov Yu. A., Puzynin A. V., Vladimirov A. A., Ivanova N. V., Pugachev V. M., Dodonov V. G., Barnakov Ch. N., Manina T. S., Ismagilov Z. R., *Materials and Manufacturing Processes*. 2016. Vol. 31, No. 6. P. 739–744.
- 9 Simenyuk G. Yu., Zakharov Yu. A., Pavelko N. V., Dodonov V. G., Pugachev V. M., Puzynin A. V., Manina T. S., Barnakov Ch. N., Ismagilov Z. R., *Catal. Today*. 2015. Vol. 249. P. 220–227.
- 10 Kriger V. G., Kalenskii A. V., Zakharov Yu. A., Tshipilev V. P., *Materialovedenie*. 2006. Vol. 9. P. 14–21.
- 11 Kolmykov R. P., Obtaining and Studying the Properties of Nickel and Cobalt Nanopowders and Their Mutual system (Abstract of Candidate's Dissertation in Chemistry), Kemerovo, 2011.